Effective Rate Models for Receptors Distributed in a Layer above a Surface: Application to Cells and Biacore

Carla Wofsy*† and Byron Goldstein†

*Department of Mathematics and Statistics, University of New Mexico, Albuquerque, New Mexico 87131, and †Theoretical Biology and Biophysics Group, Theoretical Division, Los Alamos National Laboratory, Los Alamos, New Mexico 87545 USA

ABSTRACT In the Biacore biosensor, a widely used tool for studying the kinetics of ligand/receptor binding, receptors are commonly localized to the sensor surface through attachment to polymers that extend from the surface to form a layer. The importance of the polymeric layer in analyzing data is controversial. The question of the effect of a binding layer also arises in the case of ligands interacting with binding sites distributed in the extracellular matrix of cells. To identify and quantify the effects of a binding layer on the estimation of association and dissociation rate constants, we derived effective rate coefficients. The expressions show that rate constants determined under the standard assumption that binding takes place on a two-dimensional surface underestimate the true reaction rate constants by a factor that depends on the ratio of the height of the layer to the mean free path of the ligand within the layer. We show that, for typical biological ligands, receptors, cells, and Biacore conditions, the binding layer will affect the interpretation of data only if transport of the ligand in the layer is slowed substantially—by one or two orders of magnitude—relative to transport outside the layer. From existing experiments and theory, it is not clear which Biacore experiments, if any, have transport within the dextran layer reduced to such an extent. We propose a method, based on the effective rate coefficients we have derived, for the experimental determination of ligand diffusion coefficients in a polymeric matrix.

INTRODUCTION

In analyzing the binding of ligands in solution to receptors on the surface of a cell or biosensor, it is common to model the receptors as fixed or diffusing particles on a two-dimensional (2D) surface. In many experimental systems, however, receptors are distributed in a layer above a surface. In the case of cells, specific ligands bind to sites within the extracellular matrix (glycocalyx). In the Biacore (Biacore AB, Uppsala, Sweden) an optical biosensor used widely for quantitative analysis of interactions between biomolecules, receptors are often attached to polymers that form a layer on a sensor chip (Rich and Myszka, 2000).

The extent to which a binding layer affects the interpretation of Biacore data has been investigated experimentally (Karlsson and Fält, 1997; Parsons and Stockley, 1997), numerically (Schuck, 1996), and analytically (Edwards, 2001). The results we present here facilitate the analysis of Biacore experiments, resolve an apparent contradiction between earlier numerical predictions and experimental results, and provide tools for assessing and including the effect of a binding layer when ligands bind to sites on spherical cells or beads.

Our approach is based on effective rate models (reviewed in Goldstein et al., 1999). When ligands in solution bind to receptors on a surface, whether or not the receptors are distributed in a three-dimensional (3D) layer, a complete model for binding and dissociation includes transport of the ligand to the surface and reaction at the surface. However, the resulting partial differential equation (PDE) models, including diffusion and possibly convection of the ligand, are impractical as the basis for extracting reaction rate constants from binding data. Approximate models, consisting of an ordinary differential equation (ODE) with effective rate coefficients that are explicit functions of both the transport and reaction parameters, provide the basis for simple and accurate estimation of reaction rates, under a wide range of experimental conditions (e.g., Goldstein and Dembo, 1995; Myszka et al., 1998; Mason et al., 1999; Edwards et al., 1999). Here we derive effective rate coefficients for ligands binding to receptors distributed in a layer above the surface of a spherical cell or the sensor surface of a Biacore.

Effective rate coefficients for binding and dissociation within a layer modify, in a simple way, the analogous expressions for the case where binding occurs on an impenetrable surface. The modification is that the intrinsic reaction parameters, i.e., the association and dissociation rate constants, are reduced by a factor that depends on the thickness of the layer and the mean free path of the ligand in the layer (roughly, the distance a ligand travels within the layer before it binds to a receptor). If the mean free path is large relative to the height of the binding layer, then the layer can be modeled as a 2D surface. This makes sense because, in this limit, concentrations of free and bound ligand are essentially uniform in the layer. The 3D structure of the binding layer would only be important if, in the course of an experiment, gradients developed in the ligand concentration in the layer, for example, if binding occurred to a significantly greater extent at the top than at the bottom of the layer.

Submitted June 28, 2001, and accepted for publication December 28, 2001.

Address reprint requests to Byron Goldstein, Theoretical Biology and Biophysics Group, Theoretical Division, T-10, MS K710, Los Alamos National Laboratory, Los Alamos, NM 87545. Tel.: 505-667-6538; Fax: 505-665-3493; E-mail: bxg@lanl.gov.

0006-3495/02/04/1743/13 $2.00

The main conclusion for the Biacore is that, for typical ligands and experimental design, effective rate coefficients derived from a model where receptors are distributed in the dextran layer are very close to those derived under the assumption that binding takes place on an impenetrable 2D surface. The dextran layer affects the interpretation of binding data only if diffusion of the ligand within the layer is much slower than the diffusion of a typical biological molecule in the aqueous medium outside the layer (where the diffusion coefficient is expected to be between 10^{-7} and 10^{-6} cm^2/s). This result is consistent with simulations by Schuck (1996), who used a diffusion coefficient of 10^{-8} cm^2/s for a ligand inside the dextran layer and predicted gradients in the concentrations of free and bound ligand within the layer. If such gradients are pronounced, they may lead to misinterpretation of binding data. However, our result is also consistent with Biacore experiments of Karlsson and Fält (1997) and Parsons and Stockley (1997). Both groups did not detect differences in binding or dissociation between sensor chips with receptors distributed in a dextran layer and chips with receptors bound directly to the surface. Karlsson and Fält argued that parameter values used in the Schuck calculations were not characteristic of Biacore conditions.

RESULTS

General form of effective rate coefficients for binding in a layer

The role of effective rate coefficients is to provide a good approximate description of ligand/receptor binding kinetics at a surface, using an ODE of the form,

$$\frac{dB}{dt} = k_a^e R C_T - k_d^e B, \tag{1}$$

where B and R are concentrations of bound and free receptors on the surface, C_T is the bulk concentration of ligand far from the surface, k_a^e is the effective forward (association) rate coefficient, and k_d^e is the effective reverse (dissociation) rate coefficient. The concentrations of bound and free receptors, B and R, satisfy the conservation law $R + B = R_T$, where R_T is the total surface concentration of receptors, assumed to be constant for the period of the experiment being modeled. Typical units for the concentrations of reactants are cm^{-3} or nM for the ligand and cm^{-2} or nM-cm for receptors. The formulation in Eq. 1 is for monovalent receptors and ligands.

If transport of the ligand is rapid relative to the reaction at the surface, the system is in the "reaction limit," and Eq. 1 holds with the effective rate coefficients equal to the intrinsic association and dissociation rate constants, denoted by k_a and k_d. In general, effective rate coefficients are not constants; they depend on R (equivalently, on B).

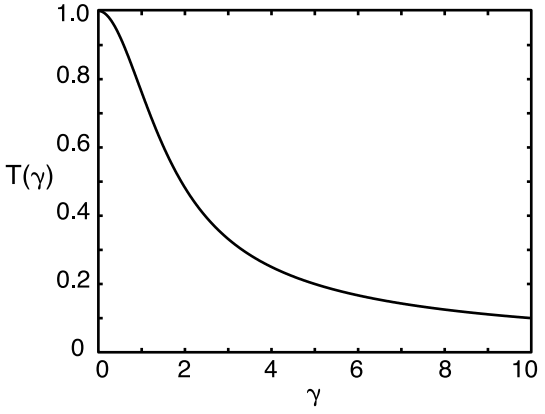

FIGURE 1 Graph of the thickness factor $T(\gamma) = \tanh(\gamma)/\gamma$ that reduces effective rate coefficients when ligand/receptor binding takes place in a 3D layer rather than on a 2D surface. When γ (Eq. 5b) is small, which occurs when the layer is thin relative to the mean free path of the ligand in the layer, then $T(\gamma) \approx 1$ and the layer has a negligible effect on binding.

For experiments where ligands bind to receptors distributed in a polymeric layer attached to the surface of a spherical cell or the sensor surface of a Biacore flow cell, we derive effective rate coefficients of the form

$$k_a^e = \frac{T(\gamma) k_a}{1 + T(\gamma) k_a R A / k_+},$$

$$k_d^e = \frac{T(\gamma) k_d}{1 + T(\gamma) k_a R A / k_+}, \tag{2}$$

which differ from those derived previously for binding to a 2D surface only in the "thickness factor" $T(\gamma)$, defined below, that multiplies the intrinsic rate constants k_a and k_d. The components of Eq. 2 are defined in the next section, where we summarize the PDE model that underlies the derivations. In brief, R is the effective surface concentration of free receptors if receptors are considered to be confined to a surface of area A, and, therefore, RA is the total number of receptors in the layer; k_+ is the transport-limited forward rate constant, i.e., the rate constant for binding to the surface, as the receptor concentration tends to ∞ and the surface becomes a perfect absorber; γ is the ratio of the height of the layer to the mean free path of the ligand in the layer, when the surface concentration of free receptors is R; and

$$T(\gamma) = \tanh(\gamma)/\gamma. \tag{3}$$

The graph of T is shown in Fig. 1. In the limit of small γ, or equivalently, when the binding layer is thin relative to the mean free path of the ligand, $T(\gamma) \approx 1$ and the effective rate coefficients approach the form expected when binding takes place on an impenetrable surface. In this case, the layer can be ignored, and binding can be modeled as occurring on a surface. When $\gamma \geq 1$, $T(\gamma)$ acts on the intrinsic reaction rates k_a and k_d as a reduction factor. In this case, if the effective rate model without the correction for the layer is

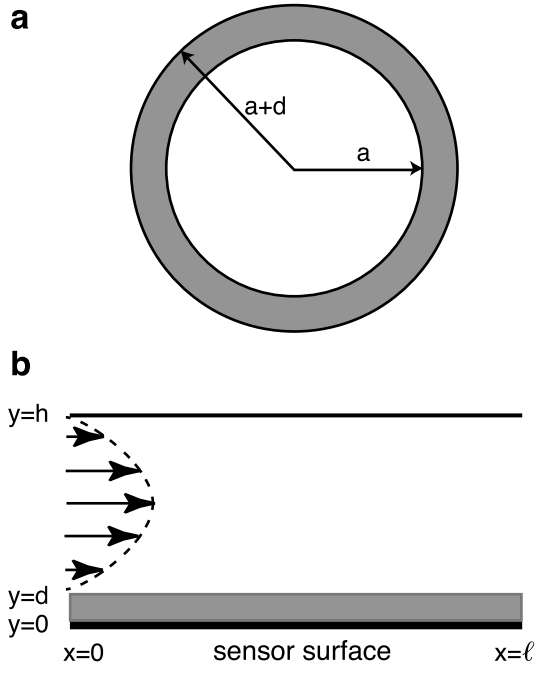

FIGURE 2 Diagrams of (*a*) a spherical cell and (*b*) the flow chamber of a Biacore biosensor, each with receptors distributed in a polymeric layer of height *d*.

used to analyze binding data, the intrinsic rate constants will be underestimated by the factor $T(\gamma)$.

Overview of the PDE model for ligand concentrations

Figure 2 sketches (*a*) a spherical cell with radius *a* and (*b*) a cross section of a Biacore flow cell, with height *h* and length *l*. In both cases, the height of the polymeric layer is *d*. The diffusion coefficient for the ligand is D_i in the layer and D_o outside. In the model for binding to a cell, transport of the ligand to the cell is by diffusion alone. For the Biacore, there is also convection, with maximum velocity v_c. In both cases, a partition coefficient Φ gives the effective fraction of the volume of the layer in which the ligand is free to diffuse. If the pore size in the polymer matrix is comparable to the size of the ligand, then the excluded volume will be greater than the volume that the polymer matrix occupies (Deen, 1987). We assume that receptors and ligands bind monovalently with intrinsic forward and reverse rate constants k_a and k_d.

In the next section, we present methods for calculating effective rate coefficients from the steady-state flux of ligands to receptors. In the model, a steady state is maintained by, in effect, replenishing ligand and receptor. This is accomplished by holding the ligand concentration, C_T, constant as the distance from the surface approaches ∞, and holding the free receptor concentration in the layer, R^{3D}, constant and uniform. (Note that we are not assuming that the free receptor concentration remains constant over time. Rather, we have a continuum of models, one for each free receptor concentration R^{3D}, that allows us to calculate effective rate coefficients for association and dissociation at each R^{3D}.) The uniformity assumption for free receptors is a substantive simplification, as discussed further below.

For the rectangular geometry of the Biacore, the effective surface concentration of free receptors satisfies

$$R = R^{3D}d. \tag{4}$$

For a spherical cell, Eq. 4 holds approximately, in the limit where the height of the layer is small relative to the radius of the cell, i.e., $d/a \ll 1$. Also, the form of the function *T* that gives the thickness factor $T(\gamma)$ in Eq. 2 has the simple form given by Eq. 3 only when $d/a \ll 1$. A typical lymphocytic cell has radius $a \approx 5 \times 10^{-4}$ cm. The extracellular matrix has height $d \approx 10^{-6}$ cm (Bongrand, 1988). Therefore, at least for these cells, $d/a \approx 2 \times 10^{-3}$ and it is reasonable to use the approximations given by Eqs. 3 and 4. (The general forms of *T* and *R* for a sphere are given in the Appendix, Eqs. A6 and A7.)

For both the spherical cell and the Biacore, the mean distance a ligand travels in the polymer layer before binding occurs (i.e., the mean free path) is

$$\bar{x} = \sqrt{D_i\Phi/(k_aR^{3D})} \tag{5a}$$

at the start of a binding experiment when all receptors are free and uniformly distributed in the layer (see Appendix). When Eq. 4 holds, in particular for the Biacore and many cell types, the mean free path can be expressed in terms of the effective surface concentration of free receptors as $\bar{x} = \sqrt{\Phi D_i d/(k_aR)}$. Then γ, the ratio of the height *d* of the layer to the mean free path of the ligand in the layer is

$$\gamma = \sqrt{\frac{k_aRd}{\Phi D_i}}. \tag{5b}$$

Consideration of the mean free path clarifies the effect of the model assumption that free receptors are distributed uniformly. In experiments, as ligands enter the layer and bind to receptors, the concentration of free receptors is depleted preferentially near the entrance to the layer. By effectively redistributing free receptors in the series of models we consider, we provide additional opportunities for binding near the entry boundary, shorten the mean free path, and consequently exaggerate the effect of the layer.

Methods for obtaining effective rate coefficients from steady-state profiles

The PDE models for the spherical cell and the Biacore flow cell presented in the Appendix determine the steady-state concentration of free ligand as a function of position, in the layer (C_i) and outside the layer (C_o). There are two equivalent ways to use the ligand concentration functions to

calculate an effective association rate coefficient. Both methods equate expressions for the total rate of binding (number of receptors bound per cell per unit time), in the effective rate ODE model and in the full PDE model. In the effective rate model, receptors that are, in fact, distributed in a layer Ω, of volume V, where the concentration of free receptors is R^{3D}, are taken to be confined to a surface with area A. The effective surface concentration of free receptors is R, where $RA = R^{3D}V$. In terms of the effective association rate coefficient k_a^e and bulk concentration of ligand, C_T, the rate of binding to the surface is

$$k_a^e R C_T A = k_a^e R^{3D} C_T V.$$

In the full model, the total rate of binding within the layer can be expressed similarly, as

$$\frac{k_a R^{3D}}{\Phi} \int_\Omega C_i \, dV,$$

so that

$$k_a^e = \frac{k_a}{\Phi} \left(\frac{1}{V} \int_\Omega \frac{C_i}{C_T} \, dV \right). \tag{6}$$

The expression for k_a^e can also be obtained from the total flux of ligand at the boundary of the binding layer, which can be expressed either in terms of C_i or C_o at the boundary. For example, in the model for binding to a sphere of radius a where the height of the layer is d, we can express C_i and C_o in terms of a radial variable r and find k_a^e from

$$k_a^e R^{3D} C_T V = A D_i \left. \frac{dC_i}{dr} \right|_{r=a+d} = A D_o \left. \frac{dC_o}{dr} \right|_{r=a+d}, \tag{7}$$

with $V = \frac{4}{3}\pi((a + d)^3 - a^3)$ and $A = 4\pi(a + d)^2$. In the Biacore model, we express ligand concentrations in terms of a height y, with $y = d$ denoting the interface between the dextran layer and the rest of the flow cell. There, $V/A = d$ and

$$k_a^e R^{3D} C_T d = D_i \left. \frac{dC_i}{dy} \right|_{y=d} = D_o \left. \frac{dC_o}{dy} \right|_{y=d}. \tag{8}$$

Once k_a^e is obtained, the effective dissociation rate coefficient, k_d^e, is defined by $k_d^e = K k_a^e$, where K denotes the equilibrium association constant, i.e., $K = k_a/k_d$. Then the effective rate model (Eq. 1) has the correct behavior at long times, as the system approaches equilibrium.

The results we obtain with these steady-state calculations agree, in the special case where a comparison is available, with an effective rate model derived by Edwards (2001, Eq. 66) from a time-dependent system of PDEs (see the discussion of Eq. A40 in the Appendix).

Effective rate coefficients for the case of a spherical cell

To evaluate the effective rate coefficients (Eq. 2) for the spherical cell, we use the diffusion-limited forward rate constant for binding to a sphere of radius $a + d$, i.e., $k_+ = 4\pi D(a + d)$ (Smoluchowski, 1917), and the corresponding surface area, $A = 4\pi(a + d)^2$. Then,

$$\frac{k_+}{A} = \frac{D_o}{a + d}. \tag{9a}$$

In the typical case where $d/a \ll 1$,

$$k_+/A \approx D_o/a. \tag{9b}$$

In summary, an approximate model that can be used to analyze binding and dissociation data from spherical cells is (Eq. 1)

$$\frac{dB}{dt} = \frac{T(\gamma)}{1 + T(\gamma) k_a R a / D_o} (k_a R C_T - k_d B), \tag{10}$$

where $R = R_T - B$.

Effective rate coefficients for the Biacore

For the Biacore flow cell, if the transport-limited forward rate constant, k_+, is expressed as a function of the distance x from the inlet of the flow cell, then (Lok et al., 1983)

$$\frac{k_+}{A} = \frac{k_+(x)}{A} = \frac{1}{\Gamma(4/3)} \left(\frac{4 v_c D_o^2}{9(h - d)x} \right)^{1/3}. \tag{11a}$$

If the transport-limited forward rate constant is averaged over the full length of the flow cell, then

$$\frac{k_+}{A} = \frac{\langle k_+ \rangle}{A} = \frac{1}{\Gamma(4/3)} \left(\frac{3 v_c D_o^2}{2(h - d)l} \right)^{1/3}. \tag{11b}$$

Eqs. 11a, 11b, or the intermediate form obtained by averaging over a portion of the flow cell are substituted into Eq. 2 to give effective rate coefficients.

In the Appendix, we consider two limits in which modified expressions for effective rate coefficients (Eqs. A36, A37, A40, A41) give marginally more accurate approximations than Eq. 2, relative to exact expressions obtained from flux calculations. However, the approximations in Eq. 2 differ by no more than 2% from the exact expressions (see Eqs. A32 and A39) for all sets of parameters and experimental conditions.

Under what conditions can the layer be neglected?

The effective rate coefficients (Eq. 2) reduce to the form obtained by treating the layer as a 2D surface when $T(\gamma) \approx 1$, or equivalently, when $\gamma \ll 1$. Because γ (Eq. 5b) is

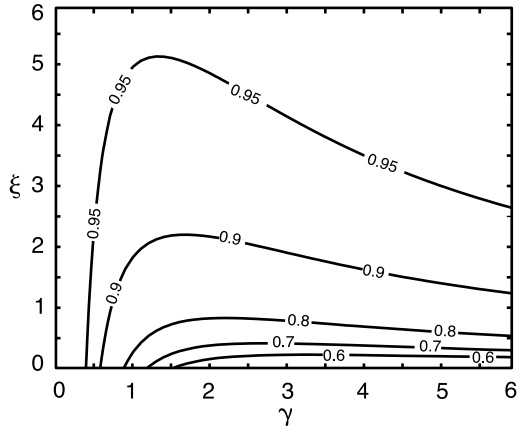

FIGURE 3 Contour curves for the ratio ρ (Eq. 13) of the effective association rate coefficients calculated with and without accounting for the binding layer. The effective rate coefficients are given by Eq. 2. The thickness factor $T(\gamma)$ corrects for the binding layer. When the binding layer is replaced by a 2D surface, $T(\gamma) = 1$. The ratio is considered as a function of $\gamma = \sqrt{k_a R d/(\Phi D_i)}$ and $\xi = \Phi D_i A/(dk_+)$. The contours show pairs of γ, ξ values for which the ratio of effective rate coefficients is 0.95, 0.9, 0.8, 0.7, or 0.6, corresponding to maximum percentage differences from 5% to 40%.

largest at the start of a binding experiment, when all receptors are free (i.e., $R = R_T$), a sufficient condition for modeling the layer as a 2D surface is

$$\sqrt{\frac{k_a R_T d}{\Phi D_i}} \ll 1. \tag{12}$$

That is, we can neglect the layer if the mean free path of the ligand in the layer, when most receptors are free, is long relative to the height of the layer.

There is an additional situation where the thickness factor T is not important in predicting binding or in fitting kinetic data, even though $T < 1$. In the transport limit, i.e., when $T(\gamma)k_a RA/k_+$ is large ($\gg$1), the dependence of k_a^e on T is negligible, because $k_a^e \approx k_+/(RA)$.

To determine conditions under which the correction for the binding layer changes effective rate coefficients by more than a specified amount, we considered the ratio ρ of effective rate coefficients with and without $T(\gamma)$ (i.e., using $T(\gamma) = 1$ for the case where the layer is ignored),

$$\rho = \frac{T(\gamma)/(1 + T(\gamma)k_a RA/k_+)}{1/(1 + k_a RA/k_+)}. \tag{13}$$

Eq. 13 shows that ρ can be written as a function of two variables. We will find it useful to consider ρ as a function of γ and a quantity $\xi = \Phi D_i A/(dk_+)$ that depends on geometric and transport-related parameters but does not depend on k_a and R. Figure 3 shows level curves of the ratio of effective rate coefficients, ρ. The contour where $\rho = 0.9$ shows that, for effective rate coefficients with and without the correction for the layer to differ by more than 10%, we must have both

$$\gamma = \sqrt{\frac{k_a R d}{\Phi D_i}} > 0.5, \tag{14a}$$

$$\xi = \frac{\Phi D_i A}{dk_+} < 2. \tag{14b}$$

The second restriction is very stringent. In the case of a spherical cell with $d/a \approx 2 \times 10^{-3}$, as estimated for typical lymphocytes, we have $k_+/A \approx D_o/a$ (Eq. 9b) and therefore we would need to have

$$\Phi D_i \le 4 \times 10^{-3} D_o, \tag{15}$$

i.e., ΦD_i would have to be at least 250-fold lower than D_o for the extracellular matrix to make a difference of more than 10% in the effective rate coefficients.

For the Biacore, in the case where $k_+ = \langle k_+ \rangle$ (Eq. 11b), Eq. 14b becomes

$$\frac{\Phi D_i}{d} \le 2\,\frac{1}{\Gamma(4/3)}\left(\frac{3 v_c D_o^2}{2(h-d)l}\right)^{1/3}. \tag{16}$$

If the layer does not retard diffusion significantly (i.e., if $D_i \approx D_o$) and does not reduce significantly the volume fraction of the layer available for reaction (i.e., if $\Phi \approx 1$), then, from Eq. 16, a necessary condition for the layer to make a difference of 10% or more in the effective rate coefficients is that the diffusion coefficient for the ligand outside the layer, D_o, satisfy

$$D_o \le \frac{16.85 v_c d^3}{(h-d)l}. \tag{17}$$

In the Biacore 2000 (Biacore AB), $h = 0.005$ cm and $l = 0.24$ cm. For the most commonly used sensor chip, CM5, $d = 10^{-5}$ cm (Karlsson et al., 1994). Based on these parameters, and using a flow rate $v_c = 10$ cm/s, common in Biacore experiments, we find that we would need $D_o < 1.4 \times 10^{-10}$ cm^2/s for Eq. 17 to hold. But typical diffusion coefficients for the biological ligands of interest in Biacore experiments are in the range $10^{-7} - 10^{-6}$ cm^2/s. Therefore, transport in the layer must be slowed significantly ($D_i \ll D_o$), or the available volume in the layer reduced significantly ($\Phi \ll 1$), for the binding layer to matter in data analysis.

How much lower than D_o does ΦD_i have to be for there to be a 10% difference between effective rate coefficients in models that treat the dextran layer explicitly and those that assume that binding occurs on a surface? From Eq. 16, using the same parameters as above, we find a necessary condition to be

$$\Phi D_i \le 5 \times 10^{-8}\ \text{cm}^2/\text{s} \quad \text{if} \quad D_o = 10^{-6}\ \text{cm}^2/\text{s}, \tag{18a}$$

$$\Phi D_i \le 10^{-8}\ \text{cm}^2/\text{s} \quad \text{if} \quad D_o = 10^{-7}\ \text{cm}^2/\text{s}. \tag{18b}$$

In the first case, transport has to be at least 20 times slower in the layer than outside. In the second case, which would correspond to very large asymmetric ligands (see Tanford, 1961, Table 21-1, p. 358), transport has to be slowed 10-fold for the layer to matter.

Recently, the height of the flow chamber (h) has been reduced to speed transport to the sensor surface (Rich and Myszka, 2000). In the Biacore 3000 (Biacore AB), $h = 2 \times 10^{-3}$ cm. This expands only slightly the range of parameter values for which the layer is expected to produce observable effects on the binding kinetics.

Proposal for quantifying ligand transport in a dextran layer

Under what experimental conditions is transport in the dextran layer reduced to the extent where we have concluded that the layer must be taken into account to estimate reaction rate constants accurately (Eqs. 14a and 14b)? Existing theory does not provide a reliable way to estimate the quantity ΦD_i that characterizes transport in the dextran layer (Yarmush et al., 1996). Here we propose a way to use experiments like those of Karlsson and Fält (1997), comparing ligand–receptor binding kinetics on sensor chips with and without a dextran layer, in conjunction with the effective rate coefficients we have derived, to estimate ΦD_i in prototypic cases. The results can be used to test models for transport of macromolecules in a polymeric matrix and to provide reasonable estimates of ΦD_i for Biacore experiments similar to the prototypes.

First, we consider the implications of our theory regarding the experimental system investigated by Karlsson and Fält (1997), where the layer did not make a measurable difference. This means that at least one of the conditions for the layer to matter (Eqs. 14a and 14b) does not hold for this system. For the parameters characterizing these experiments, Eq. 14a turns out to be the more stringent condition. The ligand is a 24-kDa antigen (p24) and the immobilized receptor an anti-p24 antibody. The reaction is relatively slow, with estimated binding rate constant $k_a = 2.2 \times 10^5$ $M^{-1}s^{-1}$. We estimate that the density of active, accessible receptor binding sites, Rd in Eq. 14a, is equal to the maximal density of bound ligands, approximately 3.85×10^{-5} M^{-1} (calculated from the molecular weight of the ligand and the maximal Biacore signal of approximately 100 RU in these experiments). Then the condition given by Eq. 14a is $\Phi D_i < 3.4 \times 10^{-9}$ cm^2/s. That is, ΦD_i would have to be 300 times lower than the diffusion coefficient expected for the ligand outside the layer, $D_o = 10^{-6}$ cm^2/s, for the layer to alter effective rate coefficients by 10% or more. The fact that the layer does not matter in the experiments of Karlsson and Fält tells us that transport in the layer is not slowed 300-fold relative to transport outside the layer. For ligand/receptor pairs that react with a faster forward rate constant, we would not require such an extreme reduction of transport within the layer to see an effect of the layer. If $k_a = 10^7$ $M^{-1}s^{-1}$, Eq. 14b (or equivalently Eq. 18a) is a more stringent condition than Eq. 14a. In this case, we should see a difference in binding to sensor surfaces with and without a dextran layer if the layer reduces ligand transport 20-fold. Despite this, Parsons and Stockley (1997) also found that the presence of the dextran layer had no effect on the binding of a small protein (≈24 kDa) to DNA on sensor chip surfaces with no dextran layer, a dextran layer of height 30 nm, or a layer of height 100 nm, even though $k_a = 3 \times 10^6$ $M^{-1}s^{-1}$ and $k_a = 8 \times 10^6$ $M^{-1}s^{-1}$ for the two DNAs studied.

Although the exception rather than the rule, we anticipate that examples will be found where ligand–receptor binding exhibits different kinetics for sensor chips with and without dextran layers. In particular, in experiments with large ligands or where high receptor densities are desirable to increase the Biacore signal, transport of the ligand in the layer may be affected to the extent where we expect the layer to make a difference. In such a case, an estimate of ΦD_i is needed for the accurate estimation of intrinsic binding and dissociation rate constants (see Eqs. 2 and 5b). We propose to obtain estimates for prototype systems where an adequate signal can be measured using a nonlayered chip, so that data can be obtained both in the presence and absence of a dextran layer. From experiments using the nonlayered chip, one would determine the binding and dissociation rate constants, k_a and k_d, and the transport-limited forward rate constant, k_+, by performing a global fit of a series of kinetic curves determined for different ligand concentrations (Myszka, 1997; Myszka et al., 1997; Myszka and Morton, 1998). With these parameters known, the thickness factor T would be determined from the binding kinetics in the presence of a layer. From the value of $T(\gamma)$, one obtains the value of γ for the layer, and, from γ, the product ΦD_i (see Eqs. 3 and 5b). Estimates of ΦD_i from the prototype systems can be applied to systems with similar ligand size, ligand geometry, receptor size, and receptor density, but where, as is the common situation, the extent of ligand/receptor binding at a receptor density achievable on a nonlayered chip gives too low a signal for reliable estimation of binding parameters.

A possible complication to this approach arises because the Biacore weights the mass of a bound ligand by a factor that decays exponentially with the distance, y, the ligand is from the sensor surface. Because the decay length of the evanescent wave is 160 nm (Karlsson and Fält, 1997), a bound ligand 100 nm (d for a CM5 chip) from the sensor surface would give a signal only 0.65 that of a ligand bound at the surface. If binding is uniform in the y direction ($T(\gamma) \approx 1$) this has no effect on the interpretation of data. However, when the binding is nonuniform and ligands bind first to sites near the top of the layer and then, after these sites are filled, to sites deeper into the layer, the amount bound at the beginning of a binding experiment will be

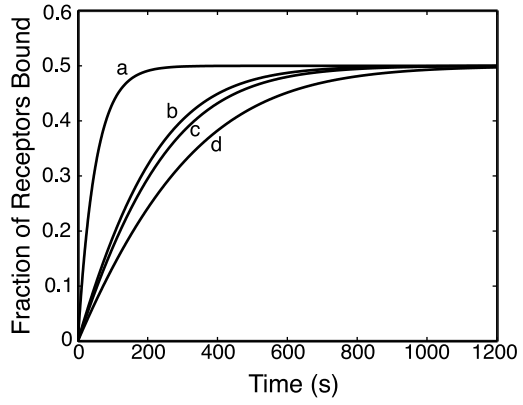

FIGURE 4 Predictions of Biacore binding, based on an effective rate model (Eq. 1), under different assumptions regarding the effective rate coefficients k_a^e and k_d^e. Curve *a* is generated using intrinsic binding and dissociation rate constants in Eq. 1 and therefore ignoring all transport effects. Curves *b*, *c*, and *d* use effective association rate coefficients given by Eq. 2, with transport-limited forward rate constant given by Eq. 11b. For all three curves, the diffusion coefficient for the ligand outside the layer is taken to be $D_o = 10^{-6}$ cm^2/s, but different assumptions are used regarding transport in the dextran layer. For curve *b*, the dextran layer is ignored, i.e., binding occurs on a 2D surface (Eq. 2 with $T(\gamma) = 1$). If we use the correction for the layer but assume that the dextran layer does not slow diffusion or reduce the effective volume in which the ligand diffuses, i.e., if $\Phi D_i = D_o$, then the predicted binding curve is essentially identical to curve *b*. In this case, the layer can be ignored. Curves *c* and *d* show the predicted binding if (*c*) $\Phi D_i = 5 \times 10^{-8}$ cm^2/s or (*d*) $\Phi D_i = 10^{-8}$ cm^2/s. The other parameters used in the simulations are in the typical range for experiments done on a Biacore 2000. The dimensions are standard for a flow cell with a CM5 chip (length $l = 0.24$ cm, height $h = 0.005$ cm, height of layer $d = 10^{-5}$ cm). We took the maximum flow rate $v_c = 10$ cm/s, the intrinsic rate constants $k_a = 0.01$ nM^{-1}s^{-1} and $k_d = 0.01$ s^{-1}, and concentrations of ligand and receptor $C_T = 1$ nM, $R_T = 1$ nM cm.

underestimated compared with the amount bound later in the experiment. As a result, under these conditions, the binding kinetics as measured by Biacore may not reflect the true binding kinetics. To get around this potential problem, a chip with a shorter dextran layer could be used to determine ΦD_i. For example, in the experiments of Parsons and Stockley (1997) a chip with $d = 30$ nm was used. A signal from a bound ligand at the top of this layer is 0.88 that of a ligand bound at the bottom.

Potential effects of slow transport of ligand in a polymeric layer

Figure 4 compares predictions of the time course of binding in a Biacore experiment, based on Eq. 1, under different assumptions regarding ligand transport. The reaction parameters are the same for all simulations. For these parameters, half of the receptors are bound at equilibrium. To compare any two predicted time courses quantitatively, we express the largest absolute difference between fractions of receptors bound as a percentage of 0.5, the maximum fraction of receptors bound in all cases. Curve *a* is obtained by using the intrinsic rate constants k_a and k_d instead of effective rate coefficients in Eq. 1, thereby ignoring transport completely, inside and outside the layer. Curves *b*, *c*, and *d*, generated using effective rate coefficients given by Eqs. 2 and 11b, predict binding when the ligand's diffusion coefficient outside the layer is $D_o = 10^{-6}$ cm^2/s. The flow rate and geometric parameters, given in the figure caption, are the same for cases *b*, *c*, and *d*. Curve *b* is obtained by setting $T(\gamma) = 1$ in Eq. 2, thereby ignoring the layer and assuming that receptors are on a 2D surface. Essentially the same curve (with values differing by at most 0.3%) is obtained using the correction for the layer but assuming ΦD_i, which determines transport in the layer, is the same as D_o. For curve *c*, $\Phi D_i = 5 \times 10^{-8}$ cm^2/s, 20-fold lower than D_o. The maximum difference from the prediction when the binding layer is ignored (or where $\Phi D_i = D_o$) is 5% in this case. Curve *d* is generated using $\Phi D_i = 10^{-8}$ cm^2/s, a factor of 100 lower than D_o. In this case, the maximum difference in predicted binding from the case where the binding layer is ignored is 16%.

The effective rate coefficients, with and without the correction for the layer, differ by 10% when $\Phi D_i = 5 \times 10^{-8}$ cm^2/s $= D_o/20$ (*case c*) and 25% when $\Phi D_i = 10^{-8}$ cm^2/s $= D_o/100$ (*case d*). These differences are greater than the corresponding differences in predicted binding (5% in case *c* and 16% in case *d*). The thickness factor $T(\gamma)$ shows an even greater effect of ignoring the correction for the dextran layer in cases *c* and *d*. The value is $T(\gamma) = 0.63$ for case *c* and $T(\gamma) = 0.32$ for case *d*. Neglecting the layer would result in significant underestimation of binding and dissociation rate constants in these cases—an estimate of $0.63k_a$ in case *c* or $0.32k_a$ in case *d*, instead of the true k_a.

DISCUSSION

For a 3D binding layer above a surface to matter in the estimation of reaction rate constants, we have shown that the average distance the ligand travels in the layer before binding occurs (i.e., the mean free path) must be comparable to, or shorter than, the height of the layer. Association and dissociation rate constants determined by methods that ignore the binding layer underestimate the true rates by a "thickness factor" T that depends on the ratio of the height of the layer to the mean free path of the ligand. The layer looks "thin" to the ligand if the mean free path is long relative to the height of the layer. In this case, $T \approx 1$. The layer is "thick" if the ligand traverses only a small fraction of the layer before binding to a receptor ($T \ll 1$). In this case, the layer may influence binding kinetics, and the interpretation of binding data, significantly. However, even under conditions where $T \ll 1$, if transport of the ligand outside the layer is so slow relative to reaction that the system is in the transport limit, the effective association and dissociation rate coefficients become independent of

the thickness factor T, and of the intrinsic reaction rate constants.

Therefore, for a reaction layer above a surface to influence binding kinetics observably, two conditions must be met. Transport of the ligand outside the layer must be fast enough relative to binding that the reaction is not transport limited. Transport in the layer must be slow enough relative to binding that gradients arise in the concentrations of free and bound ligand.

One of the conditions imposes a relation between diffusion coefficients for the ligand inside and outside the layer (see Eq. 14b). We have shown that, when ligands bind to sites in the glycocalyx of a spherical cell, diffusion of the ligand must be two orders of magnitude slower inside the glycocalyx than outside for the layer to affect the binding kinetics. For the Biacore biosensor, transport must also be substantially slower (at least an order of magnitude) inside the dextran layer than outside, for the layer to matter.

Experiments comparing ligand–receptor binding on sensor chips with and without dextran layers have failed to detect differences in the kinetics of binding (Karlsson and Fält, 1997; Parsons and Stockley, 1997). The experiments suggest that, under typical Biacore conditions, diffusion of the ligand in the layer is not so slow that the layer influences kinetic data observably. However Schuck (1996) has argued that there are plausible experimental conditions under which transport in the dextran layer is slow enough to affect Biacore data and data analysis. We have proposed a method for estimating the effective diffusion coefficient of a ligand in a dextran layer. Estimates from representative experimental systems can be used to calculate the thickness factor T in related systems, under conditions where the dextran layer is expected to matter. In such cases, the thickness factor is needed to estimate kinetic parameters accurately. Estimates of effective diffusion coefficients for ligands in a dextran layer can also be used to test models that predict macromolecular transport in a polymeric matrix.

APPENDIX

Mean free path

To calculate the mean free path a ligand travels before it becomes bound, we consider a one-dimensional steady-state problem where receptors are uniformly distributed in a layer extending from $x = 0$ to $x = \infty$. To clarify what we mean by the mean free path, picture the presence of only a single ligand whose path we follow when it moves from solution into the layer at $x = 0$. We record the distance it travels until it becomes bound, repeat this many times, and then calculate the average distance traveled. Equivalently, instead of considering only one ligand, we can consider a solution of ligands outside the layer where we hold the ligand concentration constant at the surface of the layer and we hold the concentration of free receptors constant. Because the free receptor concentration is constant, there is no competition among ligands for receptor binding sites, and the ligands move through the layer independently. Let C_o be the constant ligand concentration at $x = 0$, the boundary of the layer. Inside the layer, the ligand diffuses and is bound irreversibly so that, in the steady state inside the layer, the ligand concentration C_i obeys the equation

$$0 = D_i \frac{d^2C_i}{dx^2} - \frac{k_a R^{3D}}{\Phi} C_i.$$

The solution is

$$C_i = C_o e^{-x/\bar{x}},$$

where $\bar{x} = \sqrt{\Phi D_i/(k_a R^{3D})}$. Because $P(x) = C_i(x)/C_o$ is the probability that a ligand has not been bound between 0 and x, the mean free path $\langle x \rangle$ is

$$\langle x \rangle = \int_0^\infty P(x)\, dx = \int_0^\infty e^{-x/\bar{x}}\, dx = \bar{x}.$$

Derivations: Spherical cell

Model for a spherical cell with receptors distributed in a binding layer

The effective rate ODE model (Eqs. 1 and 2) for ligands binding to receptors distributed in a layer of height d above the surface of a spherical cell of radius a (Fig. 2 *a*) is derived from the following PDE model. As discussed in Results, calculation of effective rate coefficients comes from the steady-state flux of ligands to receptors when the free receptor concentration in the layer is R^{3D}. Additional parameters are defined in the Results section. The steady-state concentration of free ligand, at a radial distance r from the center of the cell, is denoted by $C_i(r)$ within the layer ($a < r < a + d$) and by $C_o(r)$ outside the layer ($r > a + d$). The PDEs, boundary conditions, and continuity conditions that describe the system are:

$$D_o \nabla^2 C_o = 0 \qquad a + d \le r, \qquad \text{(A1a)}$$

$$D_i \nabla^2 C_i - \frac{k_a R^{3D}}{\Phi} C_i = 0 \qquad a \le r \le a + d, \qquad \text{(A1b)}$$

$$C_o \to C_T \qquad \text{as} \quad r \to \infty, \qquad \text{(A1c)}$$

$$\frac{dC_i}{dr} = 0 \qquad \text{at} \quad r = a, \qquad \text{(A1d)}$$

$$C_i = \Phi C_o \qquad \text{at} \quad y = a + d, \qquad \text{(A1e)}$$

$$D_i \frac{dC_i}{dr} = D_o \frac{dC_o}{dr} \qquad \text{at} \quad y = a + d. \qquad \text{(A1f)}$$

In imposing the reflecting boundary condition given by Eq. A1d, we assume that the cell surface is impenetrable.

Derivation of ligand concentrations

For a radially symmetric function $C(r)$ in spherical coordinates, the Laplacian is given by

$$\nabla^2 C = \frac{1}{r^2} \frac{d}{dr} \left(r^2 \frac{dC}{dr} \right).$$

Then, solving Eq. A1a, subject to the boundary condition given by Eq. A1c, gives the following form for the ligand concentration outside the layer:

$$C_o = C_T - \frac{\alpha_o}{r} \quad a + d \le r. \qquad \text{(A2)}$$

To solve Eq. A1b for the ligand concentration in the binding layer, it is helpful to use the nondimensional variables and constants,

$$\mathrm{r} = \frac{r}{d} \qquad u = \mathrm{r}\frac{C_\mathrm{i}}{C_\mathrm{T}} \tag{A3a}$$

$$\gamma = \sqrt{\frac{k_\mathrm{a}Rd}{\Phi D_\mathrm{i}}} \qquad \delta = \frac{d}{a} \tag{A3b}$$

where R is the effective surface concentration of receptors, $R = R^{3\mathrm{D}}d$, and γ is as defined previously in Eq. 5b. Then Eq. A1b can be written as

$$\frac{\mathrm{d}^2u}{\mathrm{dr}^2} - \gamma^2 u = 0. \tag{A4}$$

The solution to Eq. A4 has the form $u(\mathrm{r}) = \alpha_\mathrm{i}\mathrm{e}^{\gamma\mathrm{r}} + \beta_\mathrm{i}e^{-\gamma\mathrm{r}}$. By the reflecting boundary condition at the cell surface (Eq. A1d), $\beta_\mathrm{i} = \alpha_\mathrm{i}e^{2\gamma/\delta}(\gamma - \delta)/(\gamma + \delta)$. Then the dimensional concentration $C_\mathrm{i}(r)$ is

$$C_\mathrm{i}(r) = \frac{C_\mathrm{T}\alpha_\mathrm{i}d}{r}\left(e^{\gamma(\mathrm{r}/\mathrm{d})} + \left(\frac{\gamma - \delta}{\gamma + \delta}\right)e^{(2\gamma/\delta)-\gamma(\mathrm{r}/\mathrm{d})}\right). \tag{A5}$$

The continuity conditions at the outer boundary of the layer (Eqs. A1e and f) determine α_i, which determines the ligand concentration C_i in the layer (Eq. A5), and α_o, which determines the ligand concentration C_o outside the layer (Eq. A2).

Derivation of effective rate coefficients

Using Eq. 6 in Results to obtain k_a^e from the total rate of ligand binding within the layer, or Eq. 7 to obtain k_a^e from the flux of ligands across the boundary of the layer, we find that k_a^e has the form given by Eq. 2 with k_+/A given by Eq. 9a. The effective surface concentration R of free receptors at the outer boundary of the layer is given by

$$\begin{aligned} R &= \frac{4/3\pi((a+d)^3 - a^3)R^{3\mathrm{D}}}{4\pi(a+d)^2} \\ &= \frac{((1+\delta)^3 - 1)}{3(1+\delta)^2\delta}R^{3\mathrm{D}}d, \end{aligned} \tag{A6}$$

and $T(\gamma)$ is replaced by a function of two variables

$$\tilde{T}(\gamma, \delta) = \left(\frac{R^{3\mathrm{D}}d}{R}\right) \times \left(\frac{e^\gamma - \left(\frac{\gamma-\delta}{\gamma+\delta}\right)e^{-\gamma}}{\gamma\left[e^\gamma + \left(\frac{\gamma-\delta}{\gamma+\delta}\right)e^{-\gamma}\right]} - \frac{\delta}{\gamma^2(1+\delta)}\right). \tag{A7}$$

In the limit $\delta \ll 1$, $R \approx R^{3\mathrm{D}}d$ and $\tilde{T}(\gamma, \delta) \approx T(\gamma)$ (Eq. 3). It is less obvious from Eq. A7, but straightforward to show by expanding in powers of γ, that, for any $\delta > 0$, the second factor in Eq. A7 approaches 1 as $\gamma \to 0$. Therefore, $\tilde{T}(\gamma, \delta)$ approaches $R^{3\mathrm{D}}d/R$ as $\gamma \to 0$ and if both γ and δ approach 0, $T(\gamma, \delta) \to 1$.

Derivations: Biacore

Biacore model, with receptors distributed in a dextran layer

In modeling flow and diffusion in a Biacore flow cell (Fig. 2 *b*), outside the dextran layer, we start with the PDE used and justified in previous models (Lok et al., 1983; Glaser, 1993; Yarmush et al., 1996; Christensen, 1997; Myszka et al., 1998; Edwards et al., 1999; Edwards, 1999; Mason et al., 1999):

$$D_\mathrm{o}\frac{\partial^2 C_\mathrm{o}}{\partial y^2} - v(y)\frac{\partial C_\mathrm{o}}{\partial x} = 0 \quad d \le y \le h, \tag{A8}$$

where h is the height of the flow cell, d is the height of the dextran layer, $C_\mathrm{o}(x, y)$ is the concentration of free analyte outside the dextran layer, D_o is the diffusion coefficient of free analyte outside the layer, and $v(y)$ is the flow velocity at height y, $d < y < h$. Two implicit, and justifiable, assumptions are that diffusion in the x direction is negligible relative to flow, and variations along the width of the flow cell are negligible, so that C_o is only a function of distance x along the length l of the flow cell and vertical distance y from the sensor surface (Mason et al., 1999).

Flow is laminar, with a parabolic velocity profile. In previous models, where the binding layer is not considered and binding is assumed to occur at the boundary $y = 0$, the velocity is given by $v(y) = 4v_\mathrm{c}(y/h)(1 - (y/h))$, where v_c is the maximum velocity. The velocity is 0 at both boundaries (i.e., at $y = 0$ and $y = h$). Then, because we are interested in the solution of Eq. A8 near $y = 0$, where binding occurs, a linear approximation of the velocity, $v(y) = 4v_\mathrm{c}(y/h)$, can be justified. The resulting linear model is the basis for effective rate approximations. In modeling the layer explicitly, we have to make a choice about how to treat flow at the boundary of the layer and within the layer. The extreme cases are that flow is the same inside and outside the dextran layer, and that there is no flow in the layer and the velocity is 0 at the boundary of the layer. Experiments indicate that the flow penetrates to some extent into the layer (Witz, 1999). We present the model where there is no flow in the layer. This is a conservative choice, in terms of determining conditions when the layer has a negligible effect on binding kinetics, because the assumption of no flow in the layer exaggerates the effect of the layer. The model is:

$$D_\mathrm{o}\frac{\partial^2 C_\mathrm{o}}{\partial y^2} - 4v_\mathrm{c}\left(\frac{y-d}{h-d}\right)\frac{\partial C_\mathrm{o}}{\partial x} = 0 \quad d \le y \le h, \tag{A9a}$$

$$D_\mathrm{i}\frac{\partial^2 C_\mathrm{i}}{\partial y^2} - \frac{k_\mathrm{a}R^{3\mathrm{D}}}{\Phi}C_\mathrm{i} = 0 \qquad 0 \le y \le d, \tag{A9b}$$

$$C_\mathrm{o} = C_\mathrm{T} \qquad \text{at} \quad x = 0, \tag{A9c}$$

$$C_\mathrm{o} \to C_\mathrm{T} \qquad \text{at} \quad y = h, \quad \text{as} \quad h \to \infty, \tag{A9d}$$

$$\frac{\partial C_\mathrm{i}}{\partial y} = 0 \qquad \text{at} \quad y = 0, \tag{A9e}$$

$$C_\mathrm{i} = \Phi C_\mathrm{o} \qquad \text{at} \quad y = d, \tag{A9f}$$

$$D_\mathrm{i}\frac{\partial C_\mathrm{i}}{\partial y} = D_\mathrm{o}\frac{\partial C_\mathrm{o}}{\partial y} \qquad \text{at} \quad y = d. \tag{A9g}$$

In terms of the nondimensional variables $\mathrm{x} = x/l$ and $y = y/h$, and constants $\delta = d/h$ and $\lambda = h\sqrt{k_\mathrm{a}R^{3\mathrm{D}}/(\Phi D_\mathrm{i})}$, the equations for the

nondimensional ligand concentration in the layer, $c_i = C_i/C_T$, and the boundary condition at the sensor surface, are (from Eqs. A9b and e):

$$\frac{\partial^2 c_i}{\partial y^2} - \lambda^2 c_i = 0 \quad 0 \le y \le \delta \tag{A10a}$$

$$\left.\frac{\partial c_i}{\partial y}\right|_{y=0} = 0. \tag{A10b}$$

The solution has the form

$$c_i(x, y) = a(x)(e^{\lambda y} + e^{-\lambda y}). \tag{A11}$$

The nondimensional ligand concentration outside the layer, $c_o = C_o/C_T$, satisfies (from Eqs. A9a and c)

$$\frac{\partial^2 c_o}{\partial y^2} - \mu(y - \delta)\frac{\partial c_o}{\partial x} = 0 \quad \delta \le y \le 1, \tag{A12a}$$

$$c_o = 1 \qquad \text{at} \quad x = 0, \tag{A12b}$$

where

$$\mu = \frac{4 v_c h^2}{l(1 - \delta) D_o}. \tag{A13}$$

Laplace transforms of ligand concentrations

To solve for c_o, we take Laplace transforms with respect to x, denoting the transform variable by s. From Eqs. A12a and b, the Laplace transform $F_o(s)$ of c_o satisfies the equation

$$\frac{\partial^2 F_o(s)}{\partial y^2} - \mu(y - \delta)(sF_o(s) - 1) = 0. \tag{A14}$$

We convert Eq. A14 to a form with a known solution by defining

$$G_o(s) = \frac{1}{s} - F_o(s), \tag{A15}$$

i.e., G_o is the Laplace transform of $1 - c_o$, and introducing the variable

$$\hat{y} = (\mu s)^{1/3}(y - \delta) \tag{A16}$$

so that Eq. A14 becomes

$$\frac{\partial^2 G_o(s)}{\partial \hat{y}^2} - \hat{y} G_o(s) = 0. \tag{A17}$$

The general solution to Eq. A17 is a linear combination of Airy functions, Ai and Bi (Abramowitz and Stegun, 1964, Section 10.4). Applying the boundary condition at $x = 0$ (Eq. A12b) and requiring that the solution remain finite as $y \to \infty$ (Eq. A9d), G_o has the form $G_o(s) = q(s)\mathrm{Ai}(\hat{y})$. Then from Eq. A15, the Laplace transform F_o of c_o has the form

$$F_o(s) = \frac{1}{s} - q(s)\mathrm{Ai}((\mu s)^{1/3}(y - \delta)). \tag{A18}$$

To apply the continuity conditions (Eqs. A9f and g), we also need the Laplace transform of c_i, $F_i(s)$. From Eq. A11, F_i has the form

$$F_i(s) = b(s)(e^{\lambda y} + e^{-\lambda y}). \tag{A19}$$

Then from Eqs. A9f and g

$$F_i(s) = \Phi F_o(s) \qquad \text{at} \quad y = \delta, \tag{A20a}$$

$$\frac{D_i}{D_o}\frac{\partial F_i}{\partial y}(s) = \frac{\partial F_o}{\partial y}(s) \quad \text{at} \quad y = \delta. \tag{A20b}$$

Application of Eqs. A20a and b determines the unknown functions $b(s)$ and $q(s)$ in Eqs. A18 and A19. In particular, to calculate an effective forward rate coefficient, we need $b(s)$,

$$b(s) = \frac{\Phi}{s\left[(e^{\lambda\delta} + e^{-\lambda\delta}) + \dfrac{\Phi\lambda(e^{\lambda\delta} - e^{-\lambda\delta})(\mu s)^{-1/3} c_1 D_i}{(c_2 D_o)}\right]}, \tag{A21}$$

where

$$c_1 = \mathrm{Ai}(0) = \frac{1}{3^{2/3}\Gamma(2/3)}, \tag{A22a}$$

$$c_2 = -\mathrm{Ai}'(0) = \frac{1}{3^{1/3}\Gamma(1/3)}. \tag{A22b}$$

Laplace transform of effective forward rate coefficient

Equating expressions for the rate of ligand/receptor binding in the layer and, effectively, at the surface (Eq. 6), we find that the effective forward rate coefficient can be expressed in terms of the nondimensional variables as

$$k_a^e(x) = \frac{k_a}{\Phi\delta}\int_0^\delta c_i(x, y)\, dy. \tag{A23}$$

The Laplace transform of $k_a^e(x)$, with respect to x, is (by Eqs. A19 and A23)

$$L\{k_a^e(x)\} = \frac{k_a b(s)}{\Phi\delta}\int_0^\delta (e^{\lambda y} + e^{-\lambda y})\, dy$$

$$= \frac{k_a b(s)}{\Phi\delta\lambda}(e^{\lambda\delta} - e^{-\lambda\delta}). \tag{A24}$$

Substituting for $b(s)$ from Eq. A21, then substituting γ (Eq. 5b) for the product $\lambda\delta$, and using the definition of T in Eq. 3, we obtain

$$L\{k_a^e(x)\} = \frac{T(\gamma)k_a}{s}\left(\frac{1}{1 + \beta s^{-1/3}}\right), \tag{A25}$$

where

$$\beta = T(\gamma)k_a R\mu^{-1/3}\left(\frac{c_1 h}{c_2 D_o}\right).$$

Using the definitions of μ, c_1, and c_2 (Eqs. A13 and A22a and b)

$$\beta = T(\gamma)k_a R\frac{\Gamma(1/3)}{\Gamma(2/3)}\left(\frac{l(h - d)}{12 v_c D_0^2}\right)^{1/3}. \tag{A26}$$

Position-dependent effective forward rate coefficient

From Eq. A25,

$$\mathrm{L}\{k_a^e(x)\} + \frac{\beta \mathrm{L}\{k_a^e(x)\}}{s^{1/3}} = \frac{T(\gamma)k_a}{s}. \qquad \text{(A27)}$$

The second term in Eq. A27 is β times the Laplace transform of the convolution of the effective forward rate coefficient, $k_a^e(x)$, and the function $x^{-2/3}/\Gamma(1/3)$. Therefore, the effective forward rate coefficient satisfies the integral equation

$$k_a^e(x) = \frac{\beta}{\Gamma(1/3)} \int_0^x k_a^e(u)(x-u)^{-2/3}\, du = T(\gamma)k_a. \qquad \text{(A28)}$$

The integral equation (Eq. A28) defines $k_a^e(x)$ implicitly. We can obtain an explicit expression for $k_a^e(x)$ in terms of convolution integrals by expressing the Laplace transform of $k_a^e(x)$ as a sum of three terms, each of which is the product of two standard Laplace transforms. The following alternative form of the Laplace transform in Eq. A25 provides the starting point

$$\mathrm{L}\{k_a^e(x)\} = \frac{T(\gamma)k_a}{\beta s^{2/3}} \left(\frac{1}{1 + (s^{1/3}/\beta)} \right). \qquad \text{(A29)}$$

Note that

$$\begin{aligned} \frac{1}{1 + (s^{1/3}/\beta)} &= \sum_{n=0}^{\infty} (-1)^n \left(\frac{s^{1/3}}{\beta} \right)^n \\ &= \sum_{k=0}^{\infty} (-1)^{3k} \left(\frac{s^k}{\beta^{3k}} \right) + \sum_{k=0}^{\infty} (-1)^{3k+1} \left(\frac{s^{k+(1/3)}}{\beta^{3k+1}} \right) \\ &\quad + \sum_{k=0}^{\infty} (-1)^{3k+2} \left(\frac{s^{k+(2/3)}}{\beta^{3k+2}} \right) \\ &= \frac{1}{1 + (s/\beta^3)} \left(1 - \frac{s^{1/3}}{\beta} + \frac{s^{2/3}}{\beta^2} \right). \end{aligned} \qquad \text{(A30)}$$

Then, from Eqs. A29 and A30,

$$\mathrm{L}\{k_a^e(x)\} = \frac{T(\gamma)k_a}{\beta^3 + s} \left(\frac{\beta^2}{s^{2/3}} - \frac{\beta}{s^{1/3}} + 1 \right). \qquad \text{(A31)}$$

It follows that the effective forward rate coefficient $k_a^e(x)$ can be expressed in terms of convolution integrals as

$$\begin{aligned} k_a^e(x) = T(\gamma)k_a \Bigg(&\frac{\beta^2}{\Gamma(2/3)} \int_0^x e^{-\beta^3(x-u)} u^{-1/3}\, du \\ &- \frac{\beta}{\Gamma(1/3)} \int_0^x e^{-\beta^3(x-u)} u^{-2/3}\, du + e^{-\beta^3 x} \Bigg). \end{aligned}$$

Making the change of variable $t = u/x$,

$$\begin{aligned} k_a^e(x) = T(\gamma)k_a e^{-\beta^3 x} \Bigg(&\frac{\beta^2 x^{2/3}}{\Gamma(2/3)} \int_0^1 e^{\beta^3 x t} t^{-1/3}\, dt \\ &- \frac{\beta x^{1/3}}{\Gamma(1/3)} \int_0^1 e^{\beta^3 x t} t^{-2/3}\, dt + 1 \Bigg). \end{aligned} \qquad \text{(A32)}$$

The integrals in Eq. A32 can be expressed in terms of Kummer functions (Abramowitz and Stegun, 1964, Eq. 13.2.1) of the form

$$M(a, a+1, z) = a \int_0^1 e^{zt} t^{a-1}\, dt, \qquad \text{(A33)}$$

with $z = \beta^3 x$ and $a = 1/3$ or $2/3$. Then

$$\begin{aligned} k_a^e(x) = T(\gamma)k_a e^{-\beta^3 x} \Bigg(&\frac{\beta^2 x^{2/3} M(2/3, 5/3, \beta^3 x)}{(2/3)\Gamma(2/3)} \\ &- \frac{\beta x^{1/3} M(1/3, 4/3, \beta^3 x)}{(1/3)\Gamma(1/3)} + 1 \Bigg). \end{aligned} \qquad \text{(A34)}$$

Equation A34 is convenient for obtaining the asymptotic behavior of $k_a^e(x)$ from the asymptotic properties of Kummer functions (see the next section). Eq. A32 is convenient for evaluating $k_a^e(x)$ numerically.

Asymptotic behavior: position-dependent case

Kummer functions of the special form in Eq. A33 have the following asymptotic properties (Abramowitz and Stegun, 1964, Eqs. 13.1.2 and 13.1.4)

$$M(a, a+1, z) \approx 1 + \frac{az}{a+1} \quad \text{as} \quad z \to 0, \qquad \text{(A35a)}$$

$$M(a, a+1, z) \approx \frac{ae^z}{z} \quad \text{as} \quad z \to \infty. \qquad \text{(A35b)}$$

If $z = \beta^3 x \ll 1$, then from Eqs. A34 and A35a,

$$\begin{aligned} k_a^e(x) &\approx T(\gamma)k_a(1 - \beta^3 x) \left(\frac{\beta^2 x^{2/3}(1 + (2/5)\beta^3 x)}{(2/3)\Gamma(2/3)} - \frac{\beta x^{1/3}(1 + (1/4)\beta^3 x)}{(1/3)\Gamma(1/3)} + 1 \right) \\ &\approx T(\gamma)k_a \left(1 - \frac{\beta x^{1/3}}{(1/3)\Gamma(1/3)} \right) \\ &\approx \frac{T(\gamma)k_a}{1 + \beta x^{1/3}/\Gamma(4/3)}. \end{aligned}$$

In terms of the dimensional distance x and the position-dependent form of the transport-limited forward rate constant given by Eq. 11a,

$$k_a^e(x) \approx \frac{T(\gamma)k_a}{1 + T(\gamma)k_aRA/(\Gamma(2/3)\Gamma(4/3)k_+(x))} \approx \frac{T(\gamma)k_a}{1 + T(\gamma)k_aRA/(1.21k_+(x))}. \quad \text{(A36)}$$

If $z = \beta^3 x \gg 1$, then Eqs. A34 and A35b yield

$$k_a^e(x) \approx T(\gamma)k_a\left[\left(\frac{\beta^2x^{2/3}}{\Gamma(2/3)}\right)\left(\frac{1}{\beta^3x}\right) - \left(\frac{\beta x^{1/3}}{\Gamma(1/3)}\right)\left(\frac{1}{\beta^3x}\right) + e^{-\beta^3x}\right]$$

$$\approx \frac{T(\gamma)k_a}{\beta x^{1/3}\Gamma(2/3)}\left[1 - \frac{\Gamma(2/3)}{\Gamma(1/3)\beta x^{1/3}}\right] \approx \frac{T(\gamma)k_a}{\beta x^{1/3}\Gamma(2/3)[1 + \Gamma(2/3)/(\Gamma(1/3)\beta x^{1/3})]} = \frac{T(\gamma)k_a}{[(\Gamma(2/3))^2/\Gamma(1/3)] + \Gamma(2/3)\beta x^{1/3}}.$$

In terms of the dimensional distance x,

$$k_a^e(x) = \frac{T(\gamma)k_a}{0.68 + T(\gamma)k_aRA/k_+(x)}. \quad \text{(A37)}$$

Effective forward rate coefficient, averaged over position

In this section, we derive an effective forward rate coefficient $\langle k_a^e\rangle$, averaged over the length of the Biacore, in terms of the average transport-limited forward rate constant $\langle k_+\rangle$ (Eq. 11b). We will find $\langle k_a^e\rangle$ by finding the Laplace transform of $\int_0^x k_a^e(u)\,du$, then inverting the transform and evaluating the resulting function at $x = 1$. Using the form of the Laplace transform of $k_a^e(x)$ given by Eq. A31,

$$L\left\{\int_0^x k_a^e(u)\,du\right\} = \frac{1}{s}L\{k_a^e(x)\} = \frac{T(\gamma)k_a}{\beta^3 + s}\left(\frac{\beta^2}{s^{5/3}} - \frac{\beta}{s^{4/3}} + \frac{1}{s}\right). \quad \text{(A38)}$$

Then $\int_0^x k_a^e(u)\,du$

$$= T(\gamma)k_ae^{-\beta^3x}\left(\frac{\beta^2}{\Gamma(5/3)}\int_0^x e^{\beta^3u}u^{2/3}\,du - \frac{\beta}{\Gamma(4/3)}\int_0^x e^{\beta^3u}u^{1/3}\,du + \int_0^x e^{\beta^3u}\,du\right).$$

Evaluating the integrals at $x = 1$ and substituting Kummer functions,

$$\langle k_a^e\rangle = T(\gamma)k_ae^{-\beta^3}\left(\frac{\beta^2M(5/3, 8/3, \beta^3)}{(5/3)\Gamma(5/3)} - \frac{\beta M(4/3, 7/3, \beta^3)}{(4/3)\Gamma(4/3)} + \frac{e^{\beta^3} - 1}{\beta^3}\right). \quad \text{(A39)}$$

Asymptotic behavior: position-averaged case

If $z = \beta^3 \ll 1$, then from Eqs. A39 and A35a,

$$\langle k_a^e\rangle \approx T(\gamma)k_a(1 - \beta^3) \times \left(\frac{\beta^2(1 + (5/8)\beta^3)}{(5/3)\Gamma(5/3)} - \frac{\beta(1 + (4/7)\beta^3)}{(4/3)\Gamma(4/3)} + 1\right) \approx T(\gamma)k_a\left(1 - \frac{\beta}{(4/3)\Gamma(4/3)}\right) \approx \frac{T(\gamma)k_a}{1 + \beta/(4/3)\Gamma(4/3)}.$$

Substituting for β from Eq. A26 yields

$$\langle k_a^e\rangle \approx \frac{T(\gamma)k_a}{1 + T(\gamma)k_aRA/(\Gamma(5/3)\Gamma(7/3)\langle k_+\rangle)} = \frac{T(\gamma)k_a}{1 + T(\gamma)k_aRA/(1.07\langle k_+\rangle)}. \quad \text{(A40)}$$

Equation A40 agrees, in the special case where the correspondence can be made, with Eq. 66 in Edwards (2001). Expressing his results in terms of our notation, he considered the limit where the Damköhler number, a ratio of characteristic velocities, is small, i.e.,

$$D_a = \frac{k_aR}{[4v_cD_o^2/((h - d)l)]^{1/3}} \ll 1.$$

In this case, from Eqs. A26 and 11b, $\beta \ll 1$, so we are in the limit where Eq. A40 holds. Edwards' Eq. 66 is an ODE for bound ligand, with coefficients expressed in terms of D_a and another ratio of velocities, D. In terms of γ (Eq. 5b) $D = \gamma^2/D_a$.

In deriving the limiting ODE, Edwards assumed implicitly that D is of lower order than $1/D_a$, so that $D_aD \ll 1$. In this limit, because $\gamma^2 = D_aD \ll 1$, our thickness factor $T(\gamma) \approx 1 - D_aD/3$. For the case where the binding signal is averaged over the full length of the sensor chip, Eq. A40 and Edwards' Eq. 66 agree to first order in D_a.

If $z = \beta^3 \gg 1$, then from Eqs. A39 and A35b,

$$\langle k_a^e\rangle \approx T(\gamma)k_a\left[\left(\frac{\beta^2}{\Gamma(5/3)}\right)\left(\frac{1}{\beta^3}\right) - \left(\frac{\beta}{\Gamma(4/3)}\right)\left(\frac{1}{\beta^3}\right) + \frac{1 - e^{-\beta^3}}{\beta^3}\right] \approx \frac{T(\gamma)k_a}{\beta\Gamma(5/3)}\left[1 - \frac{\Gamma(5/3)}{\Gamma(4/3)\beta}\right]$$

$$\approx \frac{T(\gamma)k_a}{\beta\Gamma(5/3)[1 + \Gamma(5/3)/(\Gamma(4/3)\beta)]}$$

$$= \frac{T(\gamma)k_a}{[(\Gamma(5/3))^2/\Gamma(4/3)] + \Gamma(5/3)\beta}.$$

Substituting for β gives

$$\langle k_a^e \rangle \approx \frac{T(\gamma)k_a}{0.91 + T(\gamma)k_a R/\langle k_+ \rangle}. \qquad \text{(A41)}$$

This work was supported by National Institutes of Health Grant GM35556 and National Science Foundation Grant MCB9723897 and performed in part under the auspices of the U.S. Department of Energy.

REFERENCES

Abramowitz, M., and I. A. Stegun, editors. 1964. Handbook of Mathematical Functions. National Bureau of Standards, Washington, D.C.

Bongrand, P. 1988. Physical Basis of Cell–Cell Adhesion. Chap. 10 CRC Press, Boca Raton, FL.

Christensen, L. L. H. 1997. Theoretical analysis of protein concentration determination using biosensor technology under conditions of partial mass transport limitation. *Anal. Biochem.* 249:153–164.

Deen, W. M. 1987. Hindered transport of large molecules in liquid filled pores. *AIChE. J.* 33:1409–1425.

Edwards, D. A. 1999. Estimating rate constants in a convection-diffusion equation with a boundary reaction. *IMA J. Applied Math.* 63:89–112.

Edwards, D. A. 2001. The effect of a receptor layer on the measurement of rate constants. *Bull. Math. Biol.* 63:301–327.

Edwards, D. A., B. Goldstein, and D. S. Cohen. 1999. Transport effects on surface-volume biological reactions. *J. Math. Biol.* 39:533–561.

Glaser, R. W. 1993. Antigen–antibody binding and mass transport by convection and diffusion to a surface: a two-dimensional computer model of binding and dissociation kinetics. *Anal. Biochem.* 213: 152–161.

Goldstein, B., D. Coombs, X. He, A. R. Pineda, and C. Wofsy. 1999. The influence of transport on the kinetics of binding to surface receptors: application to cells and Biacore. *J. Mol. Recog.* 12:293–299.

Goldstein, B., and M. Dembo. 1995. Approximating the effects of diffusion on reversible reactions at the cell surface: Ligand–receptor kinetics. *Biophys. J.* 68:1222–1230.

Karlsson, R., and A. Fält. 1997. Experimental design for kinetic analysis of protein–protein interactions with surface plasmon resonance biosensors. *J. Immunol. Methods.* 200:121–133.

Karlsson, R., H. Roos, L. Fägerstam, and B. Persson. 1994. Kinetic and concentration analysis using BIA technology. *Methods: A Companion to Methods Enzymol.* 6:99–110.

Lok, B. K., Y.-L. Cheng, and C. R. Robertson. 1983. Protein adsorption on crosslinked polydimethylsiloxane using total internal reflection fluorescence. *J. Colloid Interface Sci.* 91:104–116.

Mason, T., A. R. Pineda, C. Wofsy and B. Goldstein. 1999. Effective rate models for the analysis of transport-dependent biosensor data. *Math. Biosciences.* 159:123–144.

Myszka, D. G. 1997. Kinetic analysis of macromolecular interactions using surface plasmon resonance biosensors. *Curr. Opin. Biotechnol.* 8:50–57.

Myszka, D. G., X. He, M. Dembo, T. A. Morton, and B. Goldstein. 1998. Extending the range of rate constants available from Biacore: interpreting mass transport influenced binding data. *Biophys. J.* 75:583–594.

Myszka, D. G., and T. A. Morton. 1998. CLAMP: a biosensor kinetic data analysis program. *TIBS.* 23:149–150.

Myszka, D. G., T. A. Morton, M. L. Doyle, and I. M. Chaiken. 1997. Kinetic analysis of a protein antigen–antibody interaction limited by mass transport on an optical biosensor. *Biophys. Chem.* 64:127–137.

Parsons, I. D., and P. G. Stockley. 1997. Quantitation of the *Escherichia coli* methionine repressor–operator interaction by surface plasmon resonance is not affected by the presence of a dextran matrix. *Anal. Biochem.* 254:82–87.

Rich, R. L., and D. G. Myszka. 2000. Advances in surface plasmon resonance biosensor analysis. *Curr. Opin. Biotechnol.* 11:54–61.

Schuck, P. 1996. Kinetics of ligand binding to receptor immobilized in a polymer matrix, as detected with an evanescent wave biosensor. I. A computer simulation of the influence of mass transport. *Biophys. J.* 70:1230–1249.

Smoluchowski, M. V. 1917. Versuch einer mathematischen theorie der koagulationskinetik kolloider losungen. *Z. Phys. Chem.* 92:129–168.

Tanford, C. 1961. Physical Chemistry of Macromolecules. Wiley, New York.

Witz, J. 1999. Kinetic analysis of analyte binding by optical biosensors: Hydrodynamic penetration of the analyte flow into the polymer matrix reduces the influence of mass transport. *Anal. Biochem.* 270:201–206.

Yarmush, M. L., D. B. Patankar, and D. M. Yarmush. 1996. An analysis of transport resistances in the operation of Biacore: implications for kinetic studies of biospecific interactions. *Mol. Immunol.* 33:1203–1214.